The 2019 World Congress on
Advances in Structural Engineering and Mechanics (ASEM19)
Jeju Island, Korea, September 17 - 21, 2019

Study on pullout behavior of single steel fiber in SFRCC

*Saki Echizen[1)] and Toshiyuki Kanakubo[2)]

[1)] *GSSIE, University of Tsukuba, Ibaraki, 305-8573, Japan*
[2)] *Dept. of Eng. Mechanics and Energy, Univ. of Tsukuba, Ibaraki, 305-8573, Japan*
[1)] *s1820881@s.tsukuba.ac.jp*

ABSTRACT

The purpose of this study is to investigate the pullout behavior of a single steel fiber in a mortar matrix, and its influence on tensile behavior of SFRCC (Steel Fiber-Reinforced Cementitious Composite). The test parameters are the thickness of the matrix and orientation angle of fiber. The orientation angle is set by two methods, i.e., angled pullout load to specimen (called set angle), and angled fiber embedded in matrix (called embedded angle). The test results indicate that first peak load becomes greater with increasing of bond length and orientation angle. The snubbing coefficient obtained from the specimens with set angles is larger than that obtained from the specimens with embedded angle. The bridging law (tensile stress-crack width relation) is calculated using modeled pullout load – slip curves considering fiber orientation distribution.

1. INTRODUCTION

Steel Fiber-Reinforced Cementitious Composite (SFRCC) is cementitious composite with mixing short steel fibers in mortar. SFRCC improves tensile and bending characteristics of cementitious composites by bridging effect of short fibers thorough the crack after first cracking. By applying SFRCC to components in concrete structures, it is expected to improve durability and to prolong the service life of structures. However, there are few applications using SFRCC to structural elements because of the difficulty of the evaluation of bridging effect in SFRCC. Therefore, establishing the evaluation method of SFRCC is an important subject.

Previous researches have showed that the tensile performance of SFRCC is characterized by the bridging law (tensile stress-crack width relationship). The bridging law can be expressed by the sum of pullout properties of single fiber, which is based on

---
[1)] Graduate Student
[2)] Professor

fiber-matrix bond characteristic and influenced by the orientation angle of fiber (Kanakubo et al. 2016). Orientation angle is defined by two factors as shown in Fig. 1. One is that cracking surface angled against pullout direction of the fiber (Fig. 1 center, called set angle). The other one is that the fiber has angle against normal direction of cracking surface (Fig. 1 right, called embedded angle). When the fiber embedded with an orientation angle, pullout strength of the fiber in matrix increases by snubbing effect (Li et al. 1990). Snubbing effect is considered to be caused by reaction force at the bending point of the fiber, and also it depends on the quantity of matrix at the bending point of the fiber. It is considered that the difference of fiber orientation angles, such as set angle and embedded angle, causes an influence on snubbing effect.

In this study, to evaluate the influence of fiber orientation angles set by two cases, single steel fiber pullout test was conducted. By using the test results, the bridging law is calculated.

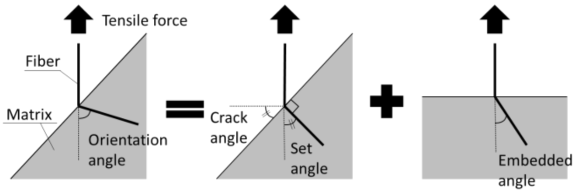

Fig. 1 Definition of set angle and embedded angle

2. OUTLINE OF PULLOUT TEST

2.1 Materials

Table. 1 shows the material properties of steel fiber. Straight steel fiber before cutting in the specified length was utilized in this study. Table 2. shows the matrix mixture proportion.

Table 1 Material properties

Fiber	Fiber diameter (mm)	Tensile strength (MPa)	Elastic modulus (GPa)
Steel	0.16	2825	210

Table 2 Mixture proportion

Water-cement ratio (%)	Unit weight(kg/m^3)				
	Water	Cement	Sand	Fly ash	Water-reducing admixture
56.0	380	678	484	291	6

2.2 Specimens

Casting mold is shown in Fig. 2 (left figure). Three rubber plates are sandwiched by two acrylic plates, and they are fixed by bolts. Molds have four holes for pouring matrix into. A punched hole has been made in the center of the mold to let the fiber go through the mortar matrix, as shown in Fig. 2 (middle figure). In case of embedded angle specimens, the upper and bottom holes have an eccentricity to ensure the initial embedded angle of fiber, as shown Fig. 2 (right figure). The parameters are specimen thickness (1mm, 2mm, 3mm, 4mm, and 6mm), orientation angle (0°, 30°, 60°) and types of orientation angle (set and embedded). Five specimens were prepared for each parameters. Bond length is calculated by specimen thickness divided by cosθ, as which θ is embedded angle.

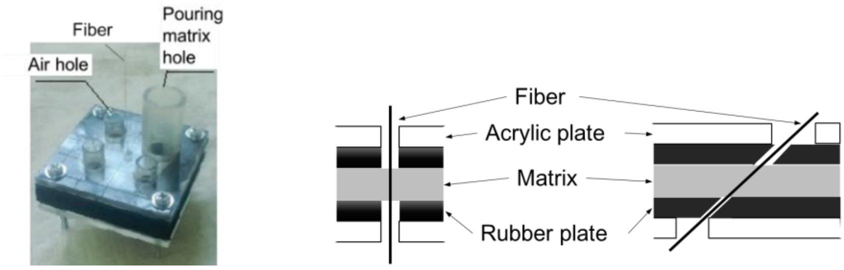

Fig. 2 Mold and its cross section

2.3 Method of loading and measurements

Pullout test was conducted using a screw-type testing machine. The measurement items for all specimens were pullout load and displacement of the loading head of the testing machine. Set angle specimens were loaded by set stand angled, as shown in Fig. 3 (left figure), embedded angle specimens were loaded as shown in Fig. 3 (right figure). Both specimens were set on the stand by steel plate bonded under the specimen.

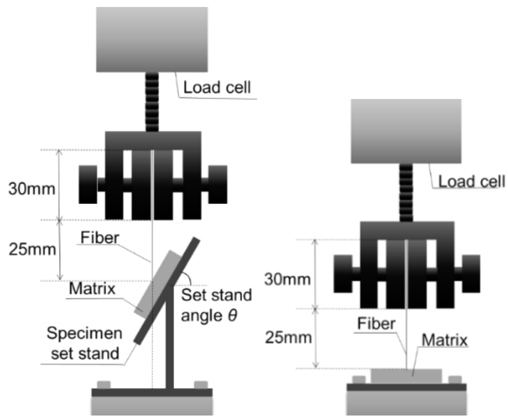

Fig. 3 Loading method

3. TEST RESULTS

Fig. 4 shows the relationships between load and slip for each specimen except fractured specimens. The case of orientation angle is noted above each graph. Slip is obtained substituting the elongation of fiber out of the matrix from the displacement of the loading head of the testing machine. The number of curves is less than five in small thickness specimens that were fractured during removing the mold.

As shown in Fig. 4, pullout load of orientation angle 0° is smaller than that of other orientation angles in same bond length. In case of orientation angle 0° specimens, pullout load increases linearly to the peak, decreases follows due to pullout of the fiber. In the other specimens, pullout load increases to the peak (first peak, P_{max}), and then keep a constant load, increases again and the fiber was pulled out completely. P_{max} is plotted in graphs.

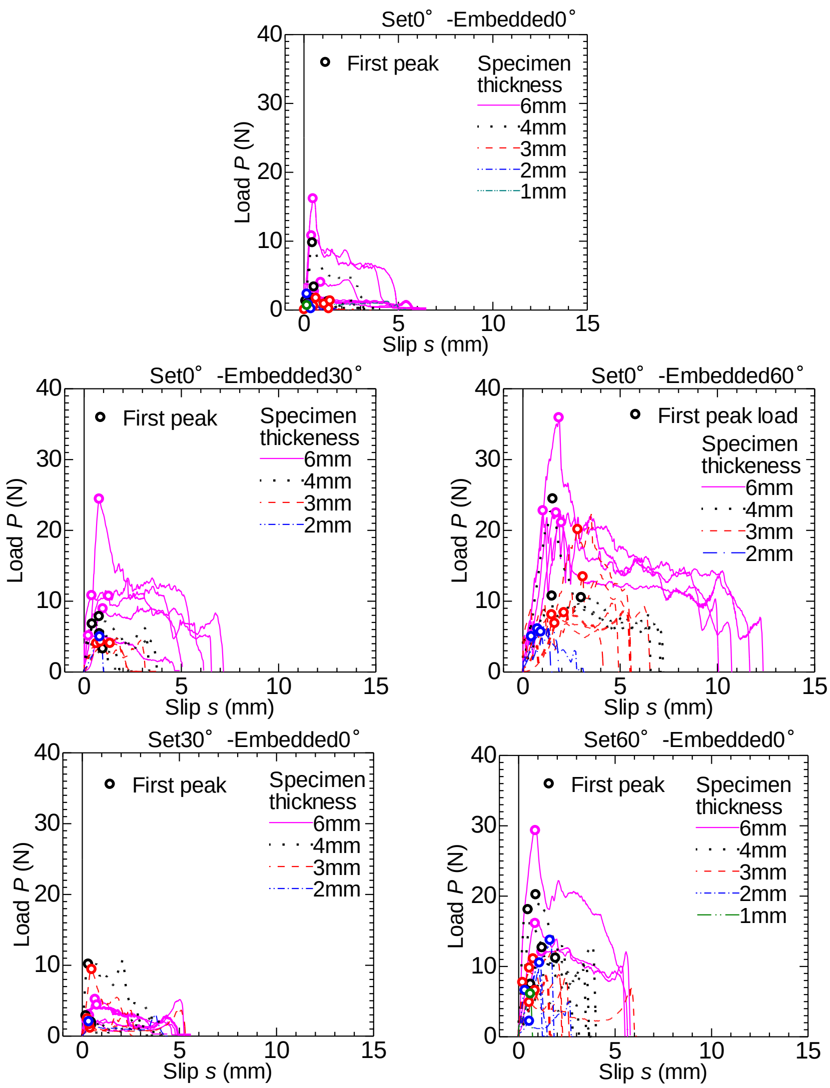

Fig. 4 Relationship between pullout load and slip

4. CALCULATION OF BRIDGING LAW

4.1 Modeling of single fiber pullout behavior

According to the pullout test results, single fiber bridging model has been modeled by bilinear model as same as the previous research (Hashimoto et al. 2016). Bilinear model represents that pullout load increases linearly to the peak, and decreases due to pullout of the fiber.

Fig. 5 shows the relationship between the first peak load and bond length, the left figure shows those in set angle specimens, and the right figure shows those in embedded angle specimens. Bond length was calculated by measured specimen thickness before loading. In each orientation angle, results are approximated by the least square method as represented by Eq.(1). $P_{1,\theta}$ represents the peak load per unit bond length at θ orientation angle.

$$P_{\max} = P_{1,\theta} \cdot l_b \tag{1}$$

The approximation results in the Fig. 5 gives that $P_{1,30}$ = 0.831(N/mm) and $P_{1,60}$ = 3.45(N/mm) in case of set angle, $P_{1,30}$ = 1.31 and $P_{1,60}$ = 2.00 for embedded angle.

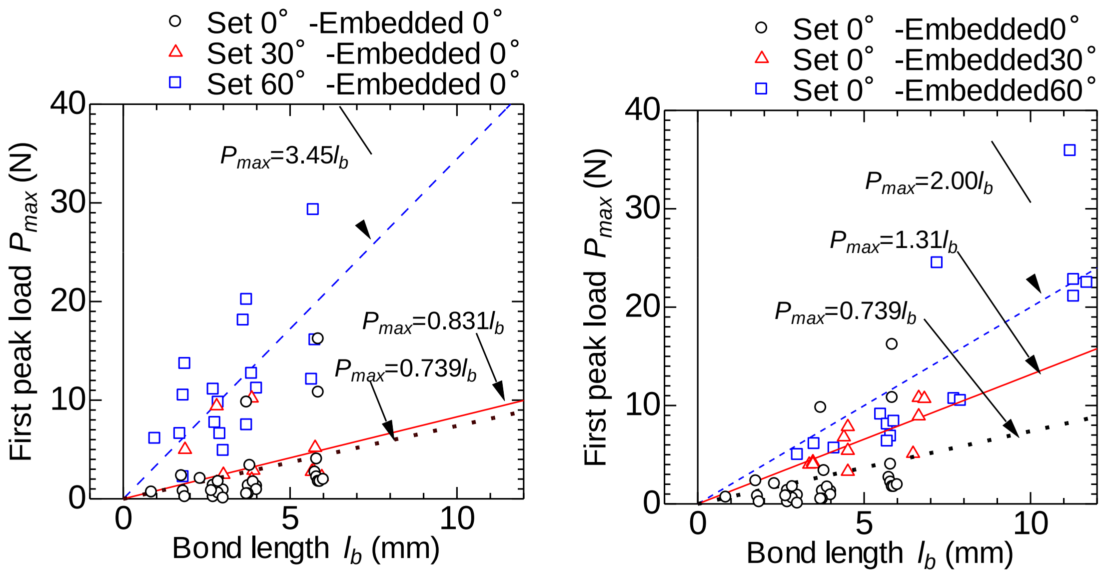

Fig.5 Relationships between first peak load and bond length
(left : set angle, right : embedded angle)

4.2 Snubbing coefficient

The snubbing effect is represented by snubbing coefficient as shown by Eq. (2).

$$P = P_0 \cdot e^{f\theta} \tag{2}$$

In Eq. (2), P is the maximum pullout load, P_0 is the maximum pullout load at 0 degree orientation angle, f is snubbing coefficient, θ is orientation angle. In this study, snubbing coefficient is calculated by the first peak load per unit bond length obtained from Fig. 5. Fig. 6 shows the relationship between the first peak load per unit bond length and orientation angle. Exponential approximations are carried out by the least square method. The results are shown as the curves in Fig. 6, which indicate the snubbing coefficients of 1.2 and 0.98 in the case of set angle and embedded angle, respectively.

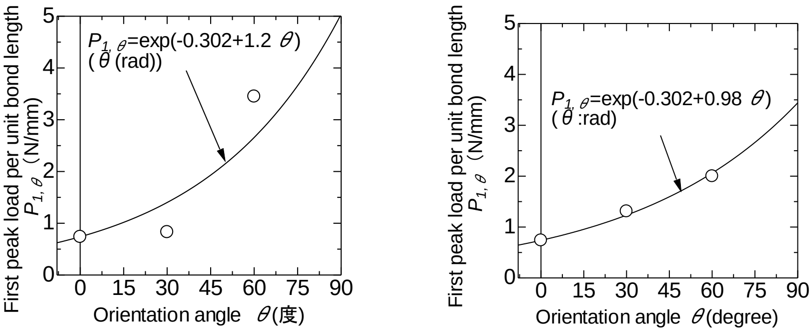

Fig. 6 Relationships between first peak load per unit bond length and orientation angle (left : set angle, right : embedded angle)

Fig. 7 shows the relationship of slip at first peak and bond length. The plots in Fig. 7 are approximated linearly by the least square method as expressed by Eq. (3).

$$s_{\max} = s_1 \cdot l_b \tag{3}$$

In Eq. (3), s_{max} is slip at first peak load, s_1 is slip at first peak load per unit bond length. The approximation result shows that s_1 is 0.19.

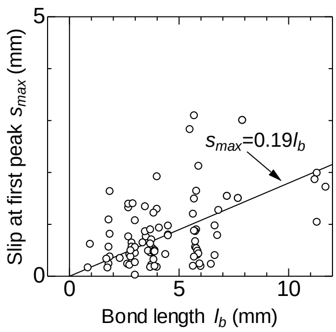

Fig. 7 Relationship between slip at first peak and bond length

To calculate the bridging law which is expressed by tensile stress-crack width relationship, the model should be given by crack width. Crack width is assumed to be two times slip by considering that the fiber is pulled out from the both ends in matrix, as given by Eq. (4).

$$\delta_{max} = 2s_{max} \tag{4}$$

By considering the influence of bond length and orientation angle, the single fiber pullout model is expressed by P_{max} and δ_{max} as Eq. (5).

$$\begin{aligned} P_{i,j}(\delta,\theta,l_b) &= \frac{P_{\max}}{\delta_{\max}}\cdot\delta \quad (\delta \leqq \delta_{max}) \\ P_{i,j}(\delta,\theta,l_b) &= P_{\max} - \frac{P_{\max}}{l_b-\delta_{\max}}\cdot(\delta-\delta_{\max}) \quad (\delta_{max}<\delta) \end{aligned} \tag{5}$$

4.3 Calculation of bridging law

In FRCC, fibers bridge across the crack as shown Fig. 8. The bridging law is calculated by applying the single fiber pullout model to each fibers. In this study, the bridging law is calculated by assuming the sectional area of 50mm x 50mm. Each fiber follows the elliptic distribution as same as previous researches (Kanakubo et al. 2016). The elliptic distribution is expressed by the orientation intensity *k* and the principal orientation angle *θr*. The principal orientation angle *θr* expresses principal orientation direction of fibers in crack plane. The orientation intensity *k* shows the fiber orientation tendency to principal orientation angle. In this study, *k* is set to 1 expressing the random orientation. The bridging law can be calculated by the sum of pullout load of each single fiber, as given by Eq. (6).

$$P(\delta) = \sum_h \sum_i \sum_j \{N_f \cdot P_{ij}(\delta,\psi,l_b)\cdot p(\theta_i)\cdot p(\phi_i)\cdot p_d(y_h,z_h)\cdot\Delta\theta\cdot\Delta\phi\cdot\Delta A\} \tag{6}$$

$P(\delta)$ = tensile force
$P_{ij}(\delta,\psi)$ = tensile force of single fiber
$P(\theta_i)$, $p(\varphi_j)$ = probability based on elliptic distribution for x-y plane and z-x plane
$P_d(y_h,z_h)$ = probability of fiber distribution along x axis (constant)
θ, φ = refer to Fig.8
N_f = number of fibers in crack plane

N_f can be expressed by Eq. (7).

$$N_f = V_f \cdot A_m / A_f \tag{7}$$

V_f = volume fraction of fiber
A_m = cross sectional area of matrix
A_f = cross sectional area of fiber

Table. 3 shows the parameters for calculation of bridging law.

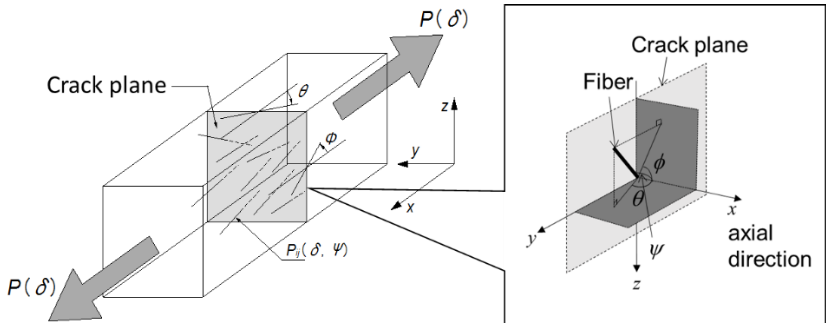

Fig. 8 Bridging fibers in crack plane

Table 3 Input parameters to calculation of bridging law

Input item	Input number	
	Embedded	Set
Cross sectional area of matrix A_m (mm^2)	50 x 50	
Fiber length l_f (mm)	13	
Snubbing coefficient f	0.98	1.2
Peak load per unit bond length at orientation angle 0 degree $P_{1,\theta}$ (N/mm)	0.739	
Crack width at first peak load per unit bond length of orientation angle 0 degree δ_1 (mm)	0.38 (0.19 x 2)	
Fiber volume fraction V_f (%)	1.0	
Orientation intensity k	1	

4.3 Result of calculation

The calculation results of tensile stress-crack width relationships are shown in Fig. 9. Tensile stress in the case of set angle is larger than that of embedded angle.

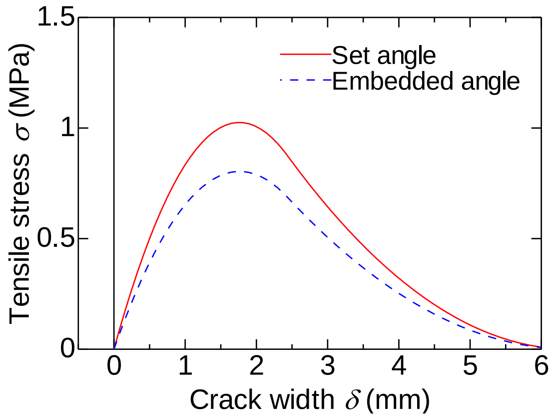

Fig. 9 Result of calculation

5. CONCLUSIONS

The result of single steel fiber pullout test shows that the snubbing coefficient in the case of set angle is larger than that of embedded angle. The results of calculation of bridging law using those snubbing coefficients show that the difference of snubbing effect causes the difference in tensile stress.

REFERENCES

Hashimoto, H., Yamada, H., Yasojima, A., Kanakubo, T., (2016) “Pullout Behavior of Steel Wire and Calculation of Bridging Law”, *Proceedings of the Japan Concrete Institute*, Vol.38, No.1, pp.249-254. (in Japanese)

Kanakubo, T., Miyaguchi, M., Asano, K., (2016) “Influence of Fiber Orientation on Bridging Performance of Polyvinyl Alcohol Fiber-Reinforced Cementitious Composeite”, *ACI Materials Journal.* Vol.113, No.2, pp.131-141.

Li, V.C., Wang, Y., Backer, S., (1990) “Effect of Inclining Angle, Bundling, and Surface Treatment on Synthetic Fiber Pull-out from a Cement Matrix”, *Composites*, Vol.**21**(2), pp.132-140